08.2

Modeling the compositional profiles across axial InSb/GaInSb/InSb nanowire heterostructures

© E.D. Leshchenko[1], V.G. Dubrovskii[2]

[1] Submicron Heterostructures for Microelectronics, Research & Engineering Center, RAS, Saint-Petersburg, Russia
[2] St. Petersburg State University, St. Petersburg, Russia
E-mail: leshchenko.spb@gmail.com

Received August 12, 2022
Revised August 12, 2022
Accepted August 17, 2022

The formation of the double InSb/GaInSb/InSb heterostructure in self-catalyzed and Au-catalyzed nanowires is studied theoretically. We calculate the compositional profiles across the axial heterostructures and study the influence of different growth parameters on the heterointerface properties, including temperature, Sb and Au concentrations.

Keywords: III-V nanowires, axial heterostructure, heterointerface, modeling

DOI: 10.21883/TPL.2022.10.54790.19339

Nanowires (NWs) and axial nanowire heterostructures based on them have several promising applications in optoelectronics and nanophotonics [1] and thus attract considerable research interest. Specifically, antimony-based NWs have found application in infrared photodetectors [2] and inverters [3]. NWs have a number of advantages, including the ability to control the morphology [4], crystal structure [5] and chemical composition [6,7] and the possibility of integration on silicon substrates [8]. Simulations of the process of formation of heterostructures based on NWs allow one to establish the relationship between their properties and growth parameters, which needs to be known for synthesis of nanostructures with controlled characteristics.

The vapor–liquid–solid growth mechanism [9] is the primary method for synthesis of axial heterostructure NWs. Owing to its versatility, gold still remains one of the most widespread catalyst elements [10]. Specifically, the possibility of growth of axial InSb/GaInSb/InSb heterostructures based on Au-catalyzed NWs has been demonstrated in [11]. However, self-catalyzed growth [12] (with a group III element contained in a growing NW serving as a catalyst) is becoming more and more common at present. This growth technique helps circumvent the unwanted incorporation of Au atoms into NWs, which leads to degradation of the optical and electronic properties of nanostructures. In addition, the self-equilibration effect on the nanowire radii [13] may be used to control the NW morphology in self-catalyzed growth. The present study is focused on modeling of the compositional profiles in a double axial InSb/GaInSb/InSb NW-based heterostructure.

Let us consider the formation of an axial heterostructure based on an NW with a droplet containing external catalyst U positioned on its tip. A BDU droplet forms after the deposition of atoms B and D, and a BD NW grows from it. The substitution of a B flux with a flux of A atoms leads to the formation of a four-component $ABDU$ solution and the growth of an $A_xB_{1-x}D$ NW. The number of atoms B in the droplet decreases with time, and the concentration of AD in the NW increases accordingly. An inverse flux substitution is needed to grow an $A_xB_{1-x}D/BD$ heterostructure. In the process of formation of monolayer i, the number of atoms A in the droplet increases through exposure to flux V_A^i and decreases due to the incorporation of atoms into the monolayer (Δ_A^i). If the contact angle and the NW radius remain constant, number N_A^i of atoms A in the droplet after the formation of monolayer i is

$$N_A^i = N_A^0 + \sum_i V_A^i - \sum_i \Delta_A^i. \quad (1)$$

Here, N_A^0 is the initial number of atoms A in the droplet ($N_A^0 = 0$). The number of atoms A incorporated into monolayer i is $\Delta_A^i = N_{\mathrm{III}}^{\mathrm{ML}} x(y^{i-1})$, where $N_{\mathrm{III}}^{\mathrm{ML}}$ is the total number of group III atoms in the monolayer, $y = c_A/(c_A + c_B)$, and c_A and c_B denote the concentrations of atoms A and B in the droplet, respectively. Next, $V_A^i = v_A \Delta t^i$, where v_A is the gas flow and Δt^i is the time interval between the moments of completion of growth of monolayers i-1 and i. If the growth rate is assumed to be linear ($\xi = rt$, where ξ is the monolayer number and r is the NW growth rate), $\Delta t^i = 1/r$. Dividing expression (1) by total number N_L of atoms in the droplet, we may present composition y^i of the droplet after the formation of monolayer i in the form

$$y^i = y_0 + \frac{g}{c_{tot}} \sum_i \left(a - x(y^{i-1})\right). \quad (2)$$

Here, $g = N_{\mathrm{III}}^{\mathrm{ML}}/N_L$ is a coefficient that depends on the material system, the NW radius, and the contact angle [14]; $a = v_A/(rN_{\mathrm{III}}^{\mathrm{ML}})$ is the dimensionless ratio of the flux of atoms A to the number of incorporated group III atoms.

Dependence $x(y)$ may be determined using various models (specifically, in the cases of nucleation-limited and

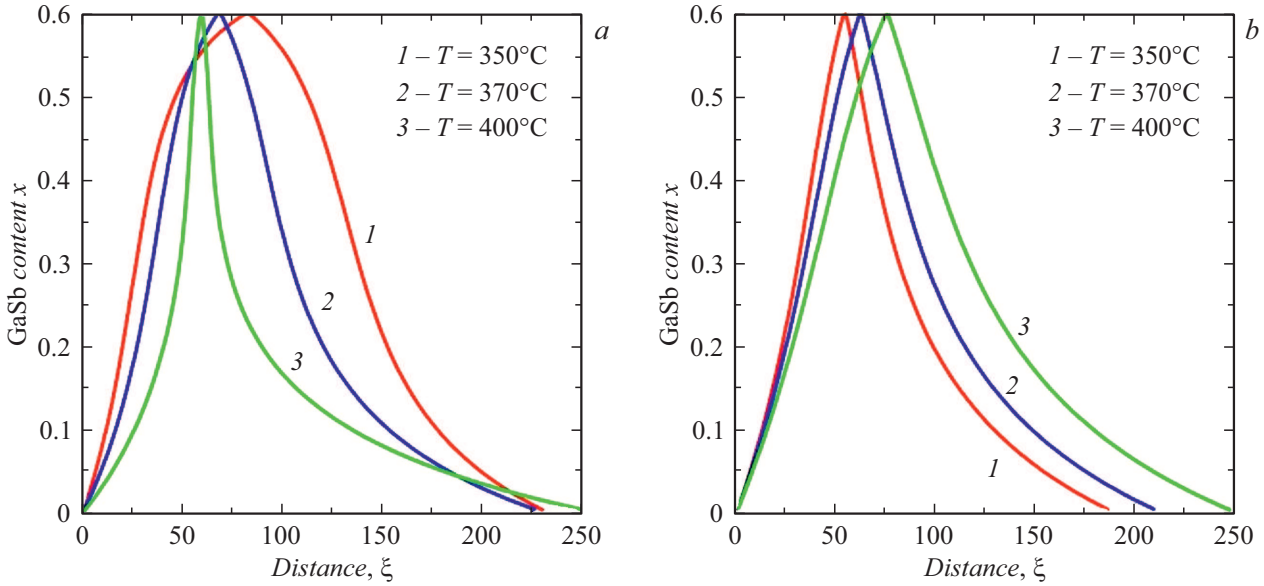

Figure 1. Compositional profiles of an NW InSb/GaInSb/InSb heterojunction calculated at different temperatures and fixed $c_{\mathrm{Au}} = 0.15$, $c_{\mathrm{Sb}} = 0.05$, $g = 0.001$, and $a = 1.2$ and 0.2 for InSb/GaInSb and GaInSb/InSb heterojunctions, respectively. *a* — Kinetic growth mode; *b* — nucleation-limited growth mode.

kinetic growth). In what follows, we use the approximation of the compositional independence of the surface energy of a nucleus [15]. The influence of composition in the case of nucleation-limited growth was considered in [16]. The nucleation-limited growth mode implies that monolayer composition x corresponds to the composition of a critical nucleus and may be written as [14,17]

$$x = \frac{1}{1 + \frac{1-y}{y} e^{-2\omega_s (x-1/2) - b}}. \qquad (3)$$

Here, ω_s is the interaction parameter between AD and BD pairs in the solid and b is a coefficient that depends on the concentrations of all elements in a droplet, the interaction parameters, and the chemical potentials of pure components [17]. We use the regular solution model and Redlich–Kister polynomials in calculations. In the kinetic mode, a monolayer grows via incorporation of AD and BD pairs in accordance with $dN_{AD}/dt = W_{AD}(1 - e^{-\Delta\mu_{AD}})$ and $dN_{BD}/dt = W_{BD}(1 - e^{-\Delta\mu_{BD}})$, where N_{AD} and N_{BD} are the numbers of AD and BD pairs in a monolayer, W_{AD} and W_{BD} are the coefficients of attachment of AD and BD pairs, and $\Delta\mu_{AD}$ ($\Delta\mu_{BD}$) is the difference between the chemical potentials of atoms A and D (B and D) in the liquid phase and the AD (BD) pair in the crystalline phase. Monolayer composition $x \equiv (dN_{AD}/dt)/(dN_{AD}/dt + dN_{BD}/dt)$ in the kinetic growth mode may be determined as

$$x = \frac{1}{1 + \frac{W_{BD}}{W_{AD}} \frac{(1 - e^{-\Delta\mu_{BD}})}{(1 - e^{-\Delta\mu_{AD}})}}. \qquad (4)$$

Let us first analyze the temperature dependence of the compositional profile of a heterojunction. The values of interaction parameters and chemical potentials were given in [17]. It can be seen from Fig. 1, *b* that a reduction in temperature leads to the formation of an NW with a sharper heterojunction in the case of nucleation-limited growth. In the kinetic growth mode (Fig. 1, *a*), an increase in T leads to the formation of a sharper InSb/GaInSb heterojunction at $x < 0.55$ widens the heterointerface at $x > 0.55$. In the case of a GaInSb/InSb heterojunction, an increase in T broadens the heterointerface (owing to a long tail in the region of $x < 0.1$). Comparing the results of two models, one sees that heterojunctions formed in the nucleation-limited growth mode are sharper than those grown in the kinetic mode; the sole exception here is the case of an InSb/GaInSb heterojunction growing at high temperatures.

Next, we consider the influence of Au concentration c_{Au} on the formation of a double heterostructure in an NW (Fig. 2). It can be seen that an increase in c_{Au} in the nucleation-limited growth mode leads to an insignificant heterojunction sharpening, which is attributable to the weakening of the reservoir effect. It follows from Fig. 2, *a* that the compositional profile of a heterojunction varies nonmonotonically in the case of kinetic growth: an increase in Au concentration translates into the formation of a more diffuse heterojunction at low c_{Au} values, but if c_{Au} increases further in the region of $c_{\mathrm{Au}} > 0.2$, a sharper heterojunction forms. This is attributable to the fact that the influence of c_{Au} on the $x(y)$ curve is stronger than the variation due to the weakening of the reservoir effect. Comparing the nucleation-limited and kinetic growth modes, one finds that the heterojunction profiles are almost matching at very low and moderate c_{Au} values.

The influence of antimony concentration c_{Sb} on the compositional profile of an axial heterojunction is presented

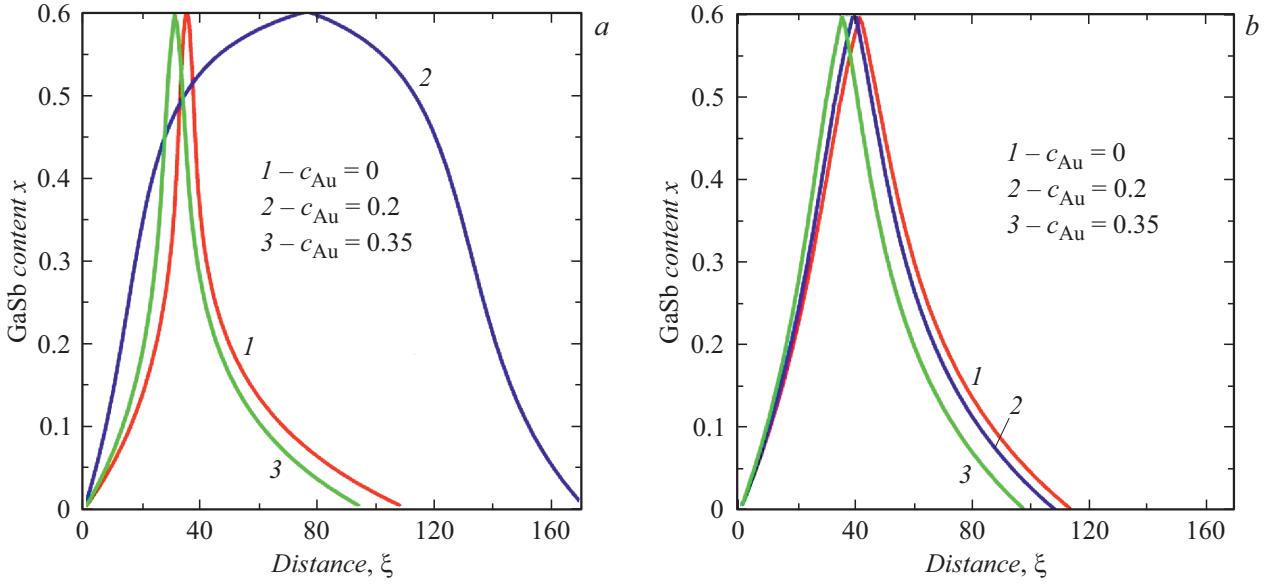

Figure 2. Compositional profiles of an NW InSb/GaInSb/InSb heterojunction calculated at different gold concentrations and fixed $T = 350^{\circ}$C, $c_{Sb} = 0.06$, $g = 0.001$, and $a = 1.5$ and 0.5 for InSb/GaInSb and GaInSb/InSb heterojunctions, respectively. *a* — Kinetic growth mode; *b* — nucleation-limited growth mode.

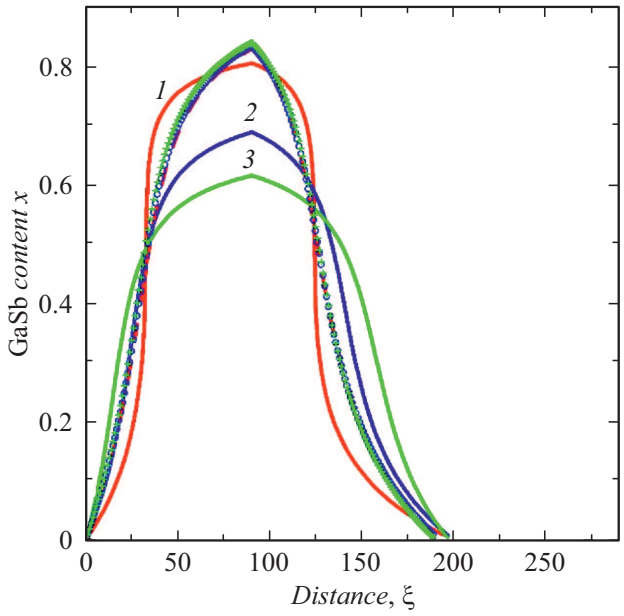

Figure 3. Compositional profiles of an NW InSb/GaInSb/InSb heterojunction calculated at different antimony concentrations and fixed $T = 350^{\circ}$C, $c_{Au} = 0.2$, $g = 0.001$, and $a = 1.5$ and 0.5 for InSb/GaInSb and GaInSb/InSb heterojunctions, respectively. $c_{Sb} = 0.025$ (solid curve *1* and dashed curve), 0.04 (solid curve *2* and circles), and 0.06 (solid curve *3* and crosses). Solid curves represent the kinetic growth mode, while the dashed curve and symbols correspond to nucleation-limited growth.

in Fig. 3. It can be seen that c_{Sb} has almost no effect on the compositional profile of a heterojunction in the nucleation-limited growth mode. The reasons for this are as follows: (1) liquid–solid composition dependence is governed by equality $\Delta\mu_{AD} = \Delta\mu_{BD}$; (2) c_{Sb} appears in chemical potential differences $\Delta\mu_{GaSb}$ and $\Delta\mu_{InSb}$ in the same form (except for the term that characterizes the excess Gibbs energy). However, since the contribution of binary and ternary interactions in a droplet is relatively small, the curves deviate only slightly from each other. In the kinetic mode, if c_{Sb} decreases from 0.06 to 0.025 by the 90th monolayer, the GaSb concentration in an NW increases from $x \approx 0.6$ to $x \approx 0.8$; i.e., a heterojunction becomes sharper. Under the given parameters, the heterojunction profile at $c_{Sb} > 0.01$ in the kinetic growth mode is sharper than the one corresponding to the nucleation-limited mode (the pattern is reverse at $c_{Sb} < 0.01$).

The developed model provides an opportunity to calculate the compositional profile of double axial heterostructures and analyze the influence of different growth parameters on the sharpness of a heterointerface. The model is applicable to any material system and any external catalyst. The obtained results may be used to optimize the parameters of growth of heterostructure NWs with sharp heterointerfaces.

Funding

V.G. Dubrovskii acknowledges financial support of analytical research within a research grant of the St. Petersburg State University (ID 93020138).

Conflict of interest

The authors declare that they have no conflict of interest.

References

[1] E. Barrigón, M. Heurlin, Z. Bi, B. Monemar, L. Samuelson, Chem. Rev., **119**, 9170 (2019). DOI: 10.1021/acs.chemrev.9b00075

[2] C.-H. Kuo, J.-M. Wu, S.-J. Lin, W.-C. Chang, Nanoscale Res. Lett., **8**, 327 (2013). DOI: 10.1186/1556-276X-8-327

[3] A.W. Dey, J. Svensson, B.M. Borg, M. Ek, L.-E. Wernersson, Nano Lett., **12**, 5593 (2012). DOI: 10.1021/nl302658y

[4] V.G. Dubrovskii, T. Xu, A.D. Alvarez, S.R. Plissard, P. Caroff, F. Glas, B. Grandidier, Nano Lett., **15**, 5580 (2015). DOI: 10.1021/acs.nanolett.5b02226

[5] K.A. Dick, P. Caroff, J. Bolinsson, M.E. Messing, J. Johansson, K. Deppert, L.R. Wallenberg, L. Samuelson, Semicond. Sci. Technol., **25**, 024009 (2010). DOI: 10.1088/0268-1242/25/2/024009

[6] M. Ghasemi, E.D. Leshchenko, J. Johansson, Nanotechnology, **32**, 072001 (2021). DOI: 10.1088/1361-6528/abc3e2

[7] B.D. Liu, J. Li, W.J. Yang, X.L. Zhang, X. Jiang, Y. Bando, Small, **13**, 1701998 (2017). DOI: 10.1002/smll.201701998

[8] G.E. Cirlin, R.R. Reznik, Yu.B. Samsonenko, A.I. Khrebtov, K.P. Kotlyar, I.V. Ilkiv, I.P. Soshnikov, D.A. Kirilenko, N.V. Kryzhanovskaya, Semiconductors, **52**, 1416 (2018). DOI: 10.1134/S1063782618110258.

[9] R.S. Wagner, W.C. Ellis, Appl. Phys. Lett., **4**, 89 (1964). DOI: 10.1063/1.1753975

[10] M.E. Messing, K. Hillerich, J. Johansson, K. Deppert, K.A. Dick, Gold Bull., **42**, 172 (2009). DOI: 10.1007/BF03214931

[11] S.G. Ghalamestani, M. Ek, K.A. Dick, Phys. Status Solidi C, **8**, 269 (2014). DOI: 10.1002/pssr.201308331

[12] P. Krogstrup, R. Popovitz-Biro, E. Johnson, M.H. Madsen, J. Nygård, H. Shtrikman, Nano Lett., **10**, 4475 (2010). DOI: 10.1021/nl102308k

[13] V.G. Dubrovskii, Phys. Rev. B, **93**, 174203 (2016). DOI: 10.1103/PhysRevB.93.174203

[14] V.G. Dubrovskii, A.A. Koryakin, N.V. Sibirev, Mater. Des., **132**, 400 (2017). DOI: 10.1016/j.matdes.2017.07.012

[15] G. Wilemski, J. Phys. Chem., **91**, 2492 (1987). DOI: 10.1021/j100294a011

[16] E.D. Leshchenko, J. Johansson, CrystEngComm, **23**, 5284 (2021). DOI: 10.1039/D1CE00743B

[17] E.D. Leshchenko, M. Ghasemi, V.G. Dubrovskii, J. Johansson, CrystEngComm, **20**, 1649 (2018). DOI: 10.1039/C7CE02201H